ORGANOMETALLICS
Article
Cite This: Organometallics XXXX, XXX, XXX–XXX
pubs.acs.org/Organometallics

Toward a Porphyrin-Style NHC: A 16-Atom Ringed Dianionic Tetra-NHC Macrocycle and Its Fe(II) and Fe(III) Complexes

Markus R. Anneser, Gaya R. Elpitiya, Xian B. Powers, and David M. Jenkins*

Department of Chemistry, University of Tennessee, Knoxville, Tennessee 37996, United States

Supporting Information

ABSTRACT: N-heterocyclic carbenes (NHCs), and macrocyclic NHCs in particular, have been applied successfully to the stabilization of high oxidation states on transition metal complexes. This access to high oxidation states has enabled their application in oxidative catalysis including aziridination and epoxidation. However, the number of macrocyclic tetra-NHC ligands is still limited, especially those featuring anionic charge, which is beneficial in this regard. In this manuscript, we report a facile and high yielding synthesis for only the second example of such a dianionic, macrocyclic tetra-NHC ligand. This 16-atom macrocycle has the ring size and charge of a porphyrin but with the increased electron donation of NHCs. Its Fe(II) and Fe(III) complexes are reported, and their reactivities for ligand addition and oxidation were tested. Multiple oxidation catalysis reactions were tested with both the Fe(II) and Fe(III) complexes with reagents such as trimethylamine-*N*-oxide, oxygen (from air), diazodiphenylmethane, and P-*tert*-butyl-dibenzo-7λ^3phosphanorbornadiene (^{t}BuPA) to explore the possibilities for single site oxidation reactions.

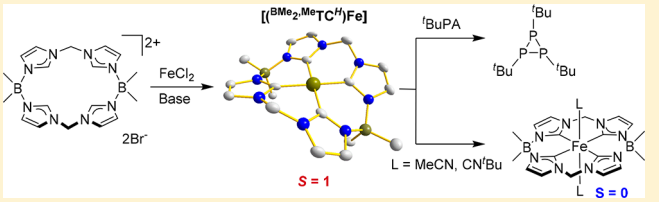

INTRODUCTION

Macrocyclic N-heterocyclic carbenes (NHCs) have gained considerable attention in organometallic chemistry for a wide variety of applications, ranging from catalysis to fluorescence.[1−12] Since their structure inherently resembles naturally occurring porphyrins, a main emphasis for research has been on their heme-analogue Fe complexes.[1,4,13,14] Indeed, several of those Fe-NHC complexes are more effective catalysts than heme analogues for oxidation reactions like aziridination and epoxidation.[15−17] Combining those traits with other known advantages of iron, such as very low toxicity, natural abundance, and low cost, the current effort put into the investigation of this type of organometallic systems is highly rational.[10]

Our group recently reported the synthesis of an 18-atom tetra-NHC macrocycle with dianionic borates in the macrocycle (Figure 1, (^{BMe_2,Et}TC^H), bottom right).[16] Overcoming the neutrality of previous NHC ligands (Figure 1, top row) for the first time has a number of beneficial effects: improved solubility,[18] increased electron donation,[18] and the first stabilization of main group metals with this class of ligand.[18−20] The iron complex of (^{BMe_2,Et}TC^H) was highly effective as an aziridination catalyst with alkyl azides.[16] Nonetheless, we are cognizant that a small change in ring size from 18- to 16-membered macrocycles can have a surprisingly severe effect on the reactivity of the coordinated metal center, as seen for metal porphyrins, and has also been demonstrated for macrocyclic NHCs by the groups of Jenkins, Meyer, and Kühn.[4,13,14,21] Thus, we desired to prepare a new dianionic, 16-membered tetra-NHC ligand that would be the most "porphyrin-like" for any macrocyclic NHC to date (Figure 1).

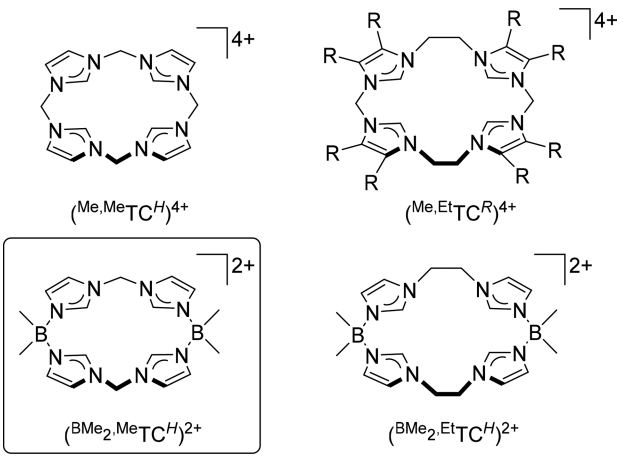

Figure 1. Selected examples of 16- and 18-membered macrocyclic imidazolium precursors that form tetra-NHCs with transition metals (R = H, Ph).[1,4,14,16] The example in the bottom left is newly reported herein.

In this paper, we showcase the synthesis of a 16-atom dianionic tetra-NHC, which is the most structurally similar to a porphyrin to date. This tetra-NHC is ligated to iron(II) and iron(III) to prepare square planar and square pyramidal complexes, respectively. Additionally, we report the reactivity of these complexes and explore some initial forays into catalytic applications. In particular, we investigated the ability

Received: December 18, 2018

DOI: 10.1021/acs.organomet.8b00923
Organometallics XXXX, XXX, XXX–XXX

for these complexes to perform single site oxidation catalysis with O, CR_2, and PR transfer reagents.

RESULTS AND DISCUSSION

The preparation of the 16-membered, dianionic, tetra-NHC precursor $(^{BMe_2,Me}TC^H)Br_2$ (**1**) can be easily achieved in excellent yields in two steps, beginning from commercial imidazole. Addition of bromodimethylborane to 1,1′-methylenediimidazole (which can be prepared from imidazole and methylene bromide)[1] in benzonitrile at 80 °C gives **1** at 95% yield as a white powder that is collected via filtration (Scheme 1). To remove residual benzonitrile, which is critical for the subsequent deprotonation steps with ^{n}BuLi,[22] we found that the best method was to repeatedly wash the powder with anhydrous THF and thoroughly dry the product under high vacuum conditions. Compound **1** was confirmed by DART MS, ^{1}H and ^{13}C NMR data, and single crystal X-ray diffraction (Figures S1, S2, and S37).

Scheme 1. Synthesis of the 16-Membered Macrocyclic Imidazolium $(^{BMe_2,Me}TC^H)Br_2$ (1)

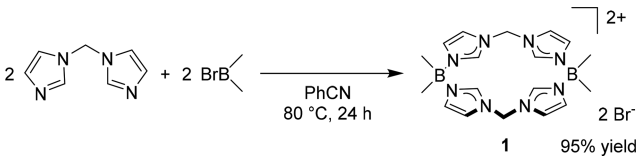

Compound **1** is air stable as a solid, but it is not stable in aqueous solution after extended exposure. Despite its instability in water, it is possible to exchange the counteranion in aqueous conditions. Dissolving **1** in a 1:2 mixture of $MeOH/H_2O$ followed by addition of aqueous KPF_6 solution (NH_4PF_6 does not work) causes immediate precipitation that replaces the bromide counterions with PF_6, which improves its solubility in organic solvents.

The synthesis of the iron complexes based on **1** was a significant challenge, since the dianionic nature of the tetra-NHC ligand impedes the deprotonation of the imidazolium precursor considerably.[4,20] The imidazolium protons' lower acidity is also reflected in the ^{1}H NMR shift of the imidazolium precursor **1** in DMSO-d_6 to 8.97 ppm (8.60 ppm for **1-PF$_6$**), which is considerably lower than that for comparable neutral compounds but higher compared to its 18-membered analogue (8.41 ppm).[16,18] These values also indicate substantial C−H···Br hydrogen bonding, as is reported for similar compounds.[19] This close interaction between Br and H is clearly seen in the single crystal X-ray of **1** (Figure S37).

Nitrogenous bases, such as LiHMDS or LDA, were ineffective, since **1** could not be deprotonated completely. Likewise, an internal base approach with $Fe(HMDS)_2{\cdot}THF$, which has been successfully applied for other cationic Fe tetra-NHC complexes, did not yield any isolable products, even under elevated temperature conditions.[4,14] In light of these failures, we turned to an even stronger base approach, ^{n}BuLi, which was effective for the 18-membered borate macrocycle.[16] Fortunately, we were able to improve upon the yields and reproducibility of this reaction, since they were previously very low for similar systems (8−25%).[16,20] The key discovery for the improvement of the synthesis was determining that even ^{n}BuLi does not readily achieve complete deprotonation of **1** and that the stability of the free tetra-NHC is modest at room temperature. Therefore, the yield and reproducibility of the iron complexes could be significantly improved by precise control of temperature and stoichiometry (Scheme 2).

Scheme 2. Synthesis of $[(^{BMe_2,Me}TC^H)Fe]$ (2) (top) and $[(^{BMe_2,Me}TC^H)FeBr]$ (3) from the 16-Membered Imidazolium Precursor $(^{BMe_2,Me}TC^H)Br_2$ (1)

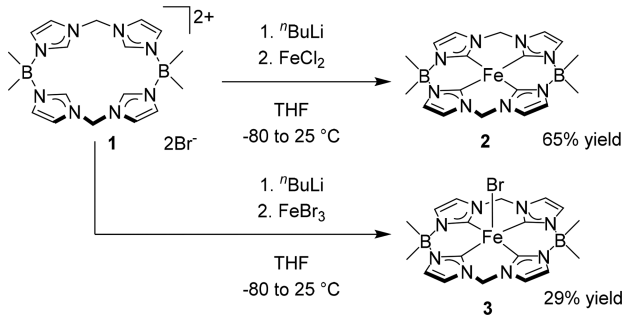

Mixing a suspension of **1** in THF with ^{n}BuLi at −80 °C does not result in complete deprotonation. Consequently, warming the reaction to 0 °C for at least 1 h is necessary to remove all of the imidazolium protons, which generates a clear yellow solution of the free tetra-NHC. All attempts to isolate this species failed, which was not unanticipated given its apparent instability. The transparent yellow carbene solution is then cooled back down to −80 °C and mixed with the iron salts, either $FeCl_2$ or $FeBr_3$, yielding the respective complexes, $[(^{BMe_2,Me}TC^H)Fe]$ (**2**) and $[(^{BMe_2,Me}TC^H)FeBr]$ (**3**), in moderate to good yields (Scheme 2). While **3** is stable even in wet and oxygenated solvent for prolonged periods of time, **2** is highly sensitive to air and moisture. This instability can be attributed to its highly unsaturated square planar coordination and its extremely low oxidation potential (*vide infra*).

A further difficulty lies in the purification of the iron complexes, since the separation of the Li-salts formed as reaction byproducts (LiBr) is not trivial. It is important to thoroughly dry the residual solids between each of the three extractions with benzene and filter over dried Celite to ensure a Li-salt-free product.

The physical characterization of **2** and **3** via cyclic voltammetry show similarities to their cationic counterparts reported previously by Kühn[4] but also the critical influence of the overall charge to the redox potentials of the Fe(II)/III) steps in these systems (+0.15 vs −0.71 V for **4**, *vide infra*). In accordance with its observed stability, **3** shows an irreversible oxidation at +360 mV and an irreversible reduction at −1250 mV in acetonitrile solution. Significantly, **3** has a lowered Fe(II/III) reduction potential by almost 300 mV compared to its 18-membered analogue ($[(^{BMe_2,Et}TC^H)FeBr]$), and thus, this smaller ligand seems to make higher oxidation states more readily available for the Fe-center.[16] Since the structures of both **2** and **3** strongly resemble Fe-porphyrins, it is reasonable that they have the same spin states as isostructural complexes. Complex **2** shows an intermediate spin of $S = 1$ and **3** a spin of $S = 1/2$ (both determined by the Evans method).[20,23,24] For **3**, the spin is independent of the solvent, but **2** will react with strong donor solvents and switch into a low-spin configuration ($S = 0$) (*vide infra*, complex **4**).

The X-ray crystal structure of **2** reveals a square planar coordinated Fe(II) center ($\tau_4 = 0.02$)[25] (Figure 2) which is isostructural to our previously reported $[(^{BMe_2,Et}TC^H)Fe]$.[16] The Fe−C bonds are on average 1.940(4) Å long, which is

DOI: 10.1021/acs.organomet.8b00923
Organometallics XXXX, XXX, XXX−XXX

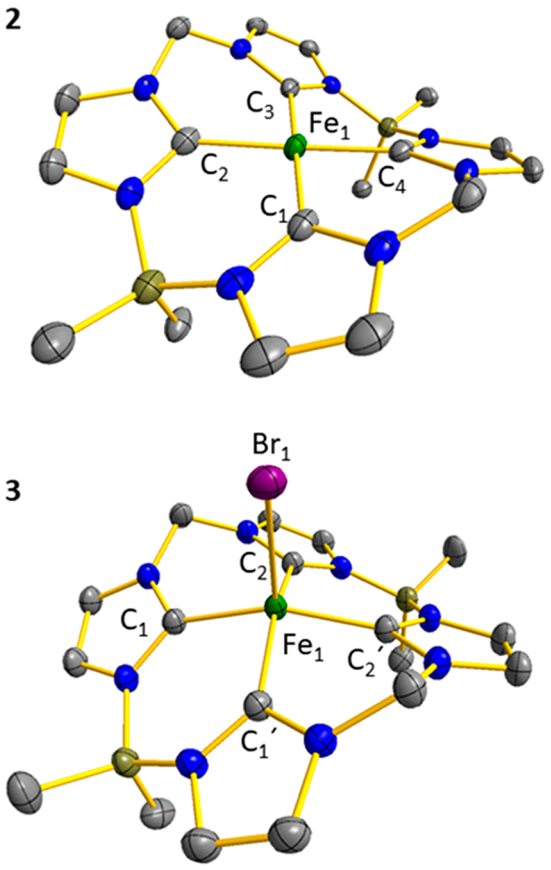

Figure 2. X-ray crystal structures of [(^{BMe_2,Me}TC^{H})Fe] (**2**) (top) and [(^{BMe_2,Me}TC^{H})FeBr] (**3**) (bottom). Green, purple, blue, gray, and olive ellipsoids (50% probability) represent Fe, Br, N, C, and B atoms, respectively. Solvent molecules and H atoms are omitted for clarity. Selected interatomic bond distances (Å) and angles (deg) are as follows: (**2**) Fe1−C1 = 1.943(3); Fe1−C2 = 1.941(3); Fe1−C3 = 1.934(3); Fe1−C4 = 1.941(3); C1−Fe1−C3 = 179.2(1); C2−Fe1−C4 = 178.3(1); (**3**) Fe1−C1 = 1.989(4); Fe1−C2 = 1.983(4); Fe1−Br1 = 2.4493(9).

slightly longer than in its dicationic, octahedral analogue, [(^{Me,Me}TC^{H})Fe]$^{2+}$ (1.908(6) Å),[4] but shorter than for its 18-membered neutral counterpart, [(^{BMe_2,Et}TC^{H})Fe] (1.989(24) Å).[16] In solution, the average symmetry of **2** is D_{2h}, reflected in the paramagnetic shifted ^{1}H NMR signals in benzene-d_6 at 12.9, 7.7, and −20.0 ppm (Figure S4). The structure of **3** shows a square pyramidal coordinated Fe(III) center with an axial bromide. The Fe−C distances are slightly longer (1.986(4) Å) compared to **2** but again shorter than in the analogous 18-membered Fe(III) complex, [(^{BMe_2,Et}TC^{H})FeBr] (2.037(16)).[16] The Fe(III) center in **3** is located 0.42 Å above the plane of the four carbene carbons, and the Fe−Br distance is 2.4493(9) Å. Despite being paramagnetic, **3** shows a characteristic set of NMR signals at room temperature in CD_3CN. The signals at +20.0, −0.2, −10.1, −24.7, and −43.8 ppm are relatively sharp and integrate to 2, 8 (2 + 6), 6, 4, and 4 H's, respectively, which demonstrates the axial asymmetry (i.e., CH_2 and BMe_2 give two peaks each) (Figure S5).

To achieve a better understanding of the electronic properties of the new ligand **1**, complex **2** was combined with the commonly used ligands MeCN, PPh_3, and CN^{t}Bu (Scheme 3) which allow for unique spectroscopic handles. All reactions took place immediately at room temperature and led

Scheme 3. Synthesis of [(^{BMe_2,Me}TC^{H})Fe(NCMe)$_2$] (4), [(^{BMe_2,Me}TC^{H})Fe(PPh_3)] (5), and [(^{BMe_2,Me}TC^{H})Fe(CN^{t}Bu)$_2$] (6) from [(^{BMe_2,Me}TC^{H})Fe] (2)

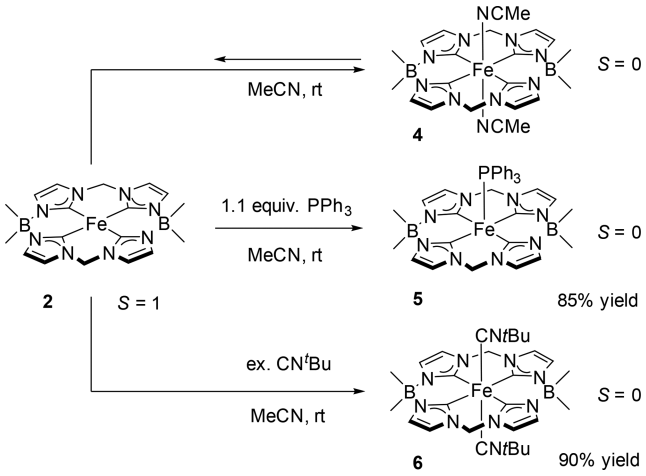

to dramatic color changes of the resulting complexes, turning the purple solution of **2** into red [(^{BMe_2,Me}TC^{H})Fe(NCMe)$_2$] (**4**), yellow [(^{BMe_2,Me}TC^{H})Fe(PPh_3)] (**5**), or green [(^{BMe_2,Me}TC^{H})Fe(CN^{t}Bu)$_2$] (**6**), respectively. The binding of the axial acetonitrile ligands in **4** is a fully reversible process and is accompanied by the change of the spin state for the Fe(II) center (S = 1 to S = 0), which was also observed for **5** and **6**. The acetonitrile ligands can be readily removed by drying in a vacuum for a short time. While the S = 0 ground state is generally observed for similar acetonitrile complexes with NHCs, they tend not to lose their axial acetonitrile ligands this easily.[1,4,14] Cyclic voltammetry measurements in MeCN for **4** show a reversible Fe(II/III) redox event at −710 mV (versus Fc), which is 860 mV less than for the dicationic analogue [(^{Me,Me}TC^{H})Fe(NCCH$_3$)$_2$]$^{2+}$ complex.[4] The previously reported [(^{BMe_2,Et}TC^{H})Fe] complex notably has a S = 1 ground state but does not bind to axial acetonitrile ligands at all, which is surprising given their structural similarity.[13] This result is interesting, since it implies that **2** may have a distinct electronic structure from either of the other reported macrocyclic tetra-NHC Fe(II) complexes which would potentially lead to different reactivity (*vide infra*).

Complexes **5** and **6** show distinct differences in reactivity and symmetry as befits their different coordination numbers and level of saturation. Phosphine adduct **5** shows the same high sensitivity to oxygen and moisture as its parent compound **2** and exhibits diamagnetic behavior in both benzene and acetonitrile. ^{1}H NMR data from complex **5** show a C_{2v} symmetry (Figure S8), indicated by the two doublets arising at 5.58/4.50 ppm and the separated signals for the CH_3 groups bound to the boron atoms (0.20/−0.14 ppm). Since the ^{31}P NMR signal at 78.7 ppm does not change in either benzene or acetonitrile, we conclude that **5** remains a square pyramidal coordination in both cases (Figure S10). Finally, there is also no evidence for the formation of a bis-phosphine complex even when a large excess of phosphine is added to **2** (10 equiv).

In a contrary manner, the smaller steric bulk of CN^{t}Bu allows for 2 equiv to bind readily to **2**, forming the symmetric, bis-substituted complex **6**. The ^{1}H and ^{13}C NMR data clearly indicate an average D_{2h} symmetry on an NMR time scale (Figures S11 and S12). ^{13}C NMR shows the shifts of the C_{NHC} signals at 191.9 ppm, which is similar to other reported Fe(II)

DOI: 10.1021/acs.organomet.8b00923
Organometallics XXXX, XXX, XXX−XXX

NHC complexes bearing isocyanide ligation.[26,27] The carbon signals of the C_{CN} atoms show up at 180.2 ppm and are broadened with no observable $^{13}C-^{14}N$ coupling.[28] The IR band of the isocyanide is observed at 2017 cm^{-1} which is comparable to the structurally similar complex reported by Song (2013 cm^{-1}).[29] Since **6** is coordinatively saturated with a strongly bound ligand, it is not surprising that it has improved stability to air and water in solution.

Reactivity of 2 with Oxidative Transfer Reagents. Since similar complexes either have been reported to form Fe(IV) oxo complexes or are highly effective for epoxidation catalysis,[14,17] we investigated the reactivity of **2** toward trimethyl *N*-oxide and molecular oxygen or air (Scheme 4).

Scheme 4. Synthesis of the $[((^{BMe_2,Me}TC^{H})Fe)_2O]$ (7) from 2 by Trimethyl *N*-Oxide or Oxygen from Air

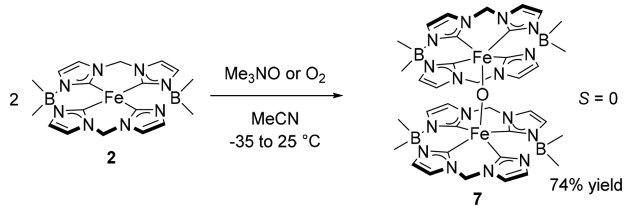

Addition of Me_3NO to **2** gave $[((^{BMe_2,Me}TC^{H})Fe)_2O]$ (**7**) in good yield and no intermediate formation of an Fe(IV) oxo species could be observed, despite it being likely the initial product of the reaction of **2** with trimethyl *N*-oxide.[14] Complex **7** is also formed if a solution of **2** is exposed to air. Not surprisingly, this makes **7** the primary impurity observed in **2**, **4**, and **5**, formed from even trace amounts of water or oxygen impurities. However, yield and purity are usually significantly diminished, compared to the pathway utilizing trimethyl *N*-oxide. Complex **7** is completely stable toward air and moisture and does not even readily act as an oxidizing agent to PPh_3,[30] yielding only 15% conversion to **5** after 4 days (Figure S15).

The structure and physical characterization of **7** are in line with similar bridging oxos and tetracarbene complexes. Complex **7** represents a strongly antiferromagnetic coupled system which yields diamagnetic ^1H and ^{13}C NMR (Figures S13 and S14). X-ray crystallography shows that the Fe1−O−Fe2 angle is 180° and the "$[(^{BMe_2,Me}TC^{H})Fe]$" fragments are twisted by 78.6° along this axis (Figure 3). The Fe−C distances are 1.967(3) Å on average and compare closely to those in **3** and other reported Fe(III) tetra-NHC complexes.[9]

Since **2** was not effective for catalytic oxygen transfer reactions, we explored viable alternatives for oxidation catalysis. Several tetra-NHC Fe(II) complexes are reported to be potent single site catalysts,[16,17,205] but none of those species are reported to show any reactivity toward potential carbene or phosphine transfer. Consequently, the reactivity of $[(^{BMe_2,Me}TC^{H})Fe]$ with "CR_2" and "PR" could be highly novel. For these reactions, we chose diazodiphenylmethane (N_2CPh_2) and P-*tert*-butyl-dibenzo-7λ^3phosphanorbornadiene (^{t}BuPA) (Scheme 5). While diazoalkanes have been studied extensively for group transfer catalysis,[31,32] there are very few reports of reactions with ^{t}BuPA.[33−35] However, stoichiometric transfers of "PR" groups reported mediated by Cr or W complexes are known.[36,37]

Test reactions with our new complexes showed catalytic degradation of N_2CPh_2 with **2** but not **3** or **7** (Table 1). At 25% catalyst loading of **2**, N_2CPh_2 is fully consumed in

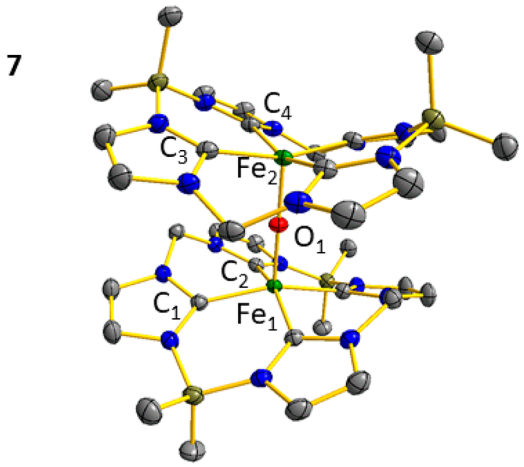

Figure 3. X-ray crystal structure of $[((^{BMe_2,Me}TC^{H})Fe)_2O]$ (**7**). Green, red, blue, gray, and olive ellipsoids (50% probability) represent Fe, O, N, C, and B atoms, respectively. Solvent molecules and H atoms are omitted for clarity. Selected interatomic bond distances (Å) and angles (deg) are as follows: (**7**) Fe1−C1 = 1.966(2); Fe1−C2 = 1.963(2); Fe2−C3 = 1.969(2); Fe2−C4 = 1.970(2); Fe1−O1 = 1.731(2); Fe2−O1 = 1.730(2); Fe1−O1−Fe2 = 180.00.

Scheme 5. Reactivity of 2 with N_2CPh_2 and ^{t}BuPA

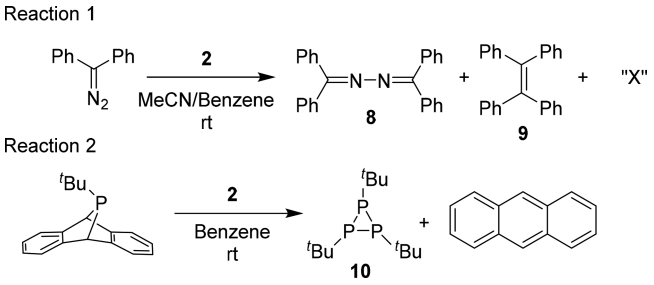

Table 1. Test Reactions with N_2CPh_2 and 2, 3, and 7

entry[a]	cat. no.	load (%)/time (h)[b]	conv.[c] (%)
1	**2**	25/1	100
2	**3**	25/24	<5
3	**7**	25/24	<5
4		-/100	~15
5	**2**	5/16	100
6	**2**	1/72	100

[a]General reaction conditions: Reactions were performed in CD_3CN or C_6D_6: 30 mg (0.15 mmol) of N_2CPh_2 was used in each run, dissolved 5 mL of the respective solvent at room temperature, and the solid catalyst was added to start the reaction. [b]Time is given after full conversion of the substrate. [c]Conversions were determined by ^1H NMR.

acetonitrile and the initial red solution turns yellow within 1 h at room temperature. Analysis of the products by ^1H and ^{13}C NMR revealed the products are a mixture of three compounds: 1,2-bis(diphenylmethylene)hydrazine (DPH, **8**), tetraphenylethene (TPE, **9**), and another unidentified compound ("X") forming in a 50/35/15 molecular ratio. Both products **8** and **9** are known side products in the decomposition of N_2CPh_2 but are usually only observed after prolonged heating in the absence of a catalyst.[38,39] Control reactions showed no reactivity toward the aforementioned products and also preceded at a much slower rate (Table 1, entry 4). Lower

DOI: 10.1021/acs.organomet.8b00923
Organometallics XXXX, XXX, XXX−XXX

catalyst loadings of 5% or even 1% showed similar results, although they naturally required prolonged reaction times to achieve complete conversion (Table 1, entries 5 and 6; Figures S16–S24). No reactions were observed when complex **3** or **7** was substituted for **2** (Table 1, entries 2 and 3). These combined findings clearly support a catalytic activity of **2** with N_2CPH_2 but with low selectivity toward the products.

For phosphinidene transfer (PR), Cummins has developed ^{t}BuPA and related compounds.[40] ^{t}BuPA reacts with **2** at a catalyst loading of 5 mol % and achieves full conversion of the substrate after only 2 h at room temperature (Table 2, entry 1). The major product of the reaction is identified as *cyclo*-$(P^tBu)_3$ (**10**) which is formed with very high selectivity and was unambiguously identified by means of ^{1}H, ^{13}C, and ^{31}P NMR (Figures S25–S30).[41] As with N_2CPh_2, no reactivity was observed between ^{t}BuPA and either **3** or **7** (Table 2, entries 2 and 3). ^{t}BuPA is quite stable in the absence of **2**, and only minor decomposition was found during a control reaction (<5%, Table 2, entry 4) after 8 h at 80 °C. Low catalyst loadings of 1 mol % of **2** showed clean conversion of ^{t}BuPA in less than 1 day at room temperature (Table 2, entry 6). Notably, the previously reported $[(^{BMe_2,Et}TC^H)Fe]$ does not show any activity in the decomposition of ^{t}BuPA, not even at 80 °C (Table 2, entry 5), again demonstrating the distinct differences in reactivity between two highly similar complexes.

Table 2. Test Reactions of 2, 3, and 7 with ^{t}BuPA

entry[a]	cat. no.	load (%)/time (h)[b]	conv.[c] (%)
1	**2**	10/2	100
2	**3**	10/24	<1
3	**7**	10/24	<1
4[d]		-/8	<5
5	*e*	10/8[e]	<5
6	**2**	1/20	100

[a]General reaction conditions: Reactions were performed in C_6D_6: 10 mg (0.04 mmol) of ^{t}BuPA was used in each run, dissolved 1 mL of C_6D_6 at room temperature, and the catalyst was added to start the reaction. [b]Time is given after full conversion of the substrate. [c]Yields were determined by ^{1}H NMR. [d]Control run at 80 °C. A similar reaction at rt showed no conversion. [e]$[(^{BMe_2,Et}TC^H)Fe]$ was used as catalyst. Reaction also heated to 80 °C.

CONCLUSION

In conclusion, we have synthesized a third generation of macrocyclic tetra-NHC ligands that moves ever closer to the structure and charge of a porphyrin but with the increased electron donation of NHCs to the transition metal. We have prepared iron complexes with this new 16-atom macrocyclic ligand in modest to good yield and demonstrated that the addition of new ligands is distinct from its previously reported 18-atom counterpart, $[(^{BMe_2,Et}TC^H)Fe]$. The iron(III) species, $[(^{BMe_2,Me}TC^H)FeBr]$, is highly stable and unreactive with oxidants, while the iron(II) species, $[(^{BMe_2,Me}TC^H)Fe]$, is highly reactive across a variety of group transfer reagents. In the case of oxygen transfer, a stable bridging oxo complex is formed from either Me_3NO or air. On the other hand, reactions of $[(^{BMe_2,Me}TC^H)Fe]$ with N_2CPh_2 and ^{t}BuPA lead to degradative catalysis of these reagents at room temperature. Diazodiphenylmethane yields 1,2-bis(diphenylmethylene)-hydrazine and tetraphenylethene as catalytic products, while ^{t}BuPA yields exclusively *cyclo*-$(P^tBu)_3$. Given the reactivity differences between the 16- and 18-atom macrocycles, we believe that a plethora of novel chemistry can be developed with this new tetra-NHC ligand.

EXPERIMENTAL SECTION

Synthesis of $(^{BMe_2,Me}TC^H)Br_2$ (1). 1,1′-Methylenediimidazole (3.85 g, 26.0 mmol) was dissolved in 150 mL of benzonitrile in a 250 mL round-bottom flask. Bromodimethylborane (6.30 g, 52.0 mmol) was pipetted into the benzonitrile solution, and the mixture was stirred for 15 min. A second portion of 1,1′-methylenediimidazole (4.45 g, 26.0 mmol) was then added into the flask. The resulting solution was brought out of the glovebox, and the reflux condenser was connected under a steady stream of N_2. The reaction mixture was heated to 80 °C and stirred for 24 h. After 24 h, the solution was cooled to 0 °C and filtered over a fine sintered-glass frit. The off-white precipitate was then washed with acetonitrile (2 × 20 mL), THF (3 × 30 mL), and diethyl ether (2 × 100 mL) and dried under reduced pressure, leaving the white product (13.2 g, 95% yield). Crystals for X-ray diffraction were grown from a solution in methanol by vapor diffusion with diethyl ether. ^{1}H NMR (DMSO-d_6, 499.74 MHz): δ 8.87 (s, 4H), 7.87 (s, 4H), 7.47 (s, 4H), 6.49 (s, 4H), 0.23 (s, 12H). ^{13}C NMR (DMSO-d_6, 125.66 MHz): δ 137.5, 123.3, 121.6, 57.2, 8.6. IR: 3106, 3056, 3010, 2933, 1550, 1536, 1304, 1262, 1366, 1304, 1252, 1136, 1108, 1087, 1049, 1020 970, 950, 880, 799, 759, 712, 689, 665, 658 cm^{-1}. DART HR MS (m/z): $[M]^{2+}$ Found: 189.1340. Calcd: 189.1306. Anal. Calcd for $C_{18}H_{28}B_2N_8Br_2$: C, 40.20; H, 5.25; N, 20.80. Found: C, 39.92; H, 5.04; N, 20.64.

Synthesis of $[(^{BMe_2,Me}TC^H)Fe]$ (2). $(^{BMe_2,Me}TC^H)Br_2$ (**1**) (3.00 g, 5.56 mmol) was suspended in 150 mL of THF in a 250 mL Schlenk flask. In a second 250 mL Schlenk flask, anhydrous $FeCl_2$ (710 mg, 5.60 mmol) was suspended in 25 mL of THF, and finally, a small Straus tube (25 mL) was filled with 9.1 mL of 2.5 M ^{n}BuLi solution in hexanes (22.8 mmol). All three flasks were taken out of the glovebox and connected to a Schlenk line. The ligand suspension and the ^{n}BuLi solution were cooled to −80 °C in an acetone/dry ice bath for 15 min. Under vigorous stirring of the solution of **1**, the ^{n}BuLi solution was added to the ligand suspension and mixed at −80 °C for at least 1 h. The now yellow suspension was allowed to warm up to 0 °C (cooled with an ice bath) and vigorously stirred for another hour or until a clear yellow solution was obtained. The clear solution was then cooled back down to −80 °C and added to the flask containing the $FeCl_2$/THF suspension, which resulted in the mixture immediately changing its color to brownish red. The mixture was allowed to slowly warm up to room temperature and was stirred overnight. The dark solution was evaporated in a 30 °C water bath (vacuum <100 mTorr) for several hours to yield a brown solid. The solid was transferred into the glovebox and extracted with benzene (3 × 50 mL) and filtered over a fine frit until the extract was no longer colored. The brownish-red benzene solution was evaporated, thoroughly dried, and again extracted with benzene at least two more times. The benzene solution was filtered over Celite over a fine frit. The solution was concentrated and layered with pentane. After several days, purple crystals were collected, washed with pentane, and dried under a vacuum. The combined yield of crystalline product was 1.55 g (3.61 mmol, 65% yield). ^{1}H NMR (C_6D_6, 499.74 MHz): δ 12.8 (4H), 7.7 (16H), −20.0 (4H). IR: 3132, 2925, 1607, 1541, 1464, 1412, 1354, 1277, 1164, 1108, 1060, 1034, 1032, 953, 815, 797, 720, 676 cm^{-1}. DART HR MS (m/z): $[M]^+$ 430.1682 (found), 430.1659 (calcd).

Synthesis of $[(^{BMe_2,Me}TC^H)FeBr]$ (3). The synthesis of **3** was performed the same way as the synthesis of **2** using anhydrous $FeBr_3$ (548 mg, 1.86 mmol), **1** (1.00 g, 1.86 mmol), and 3.1 mL of 2.5 M ^{n}BuLi solution (7.81 mmol) in hexanes. The dark green, clear solution was evaporated in a 30 °C water bath (vacuum <100 mTorr) for several hours to yield a dark solid. The solid was transferred into the glovebox, extracted with benzene, and filtered over a fine frit until the extract was no longer colored (ca. 100 mL). The greenish benzene solution was concentrated under reduced pressure to about 10 mL. The dark blue supernatant solution was separated from the yellow powder formed during the evaporation of the benzene, and the

DOI: 10.1021/acs.organomet.8b00923
Organometallics XXXX, XXX, XXX–XXX

residue was washed with a little benzene twice. The remaining yellow powder was redissolved in benzene and filtered over Celite. After drying, the yield was 280 mg (0.55 mmol, 29%). ^{1}H NMR (MeCN-d_3, 499.74 MHz): δ 20.0 (2H), −0.2 (8H), −10.1 (6H), −24.7 (4H), −43.8 (4H). IR: 3164, 3136, 2918, 1625, 1546, 1465, 1416, 1331, 1285, 1171, 1152, 1115, 1062, 1042, 952, 817, 797, 735, 682 cm^{-1}. DART HR MS (m/z): $[M-CH_3]^+$ 494.0605 (found), 494.0603 (calcd).

Synthesis of [(^{BMe_2,Me}TC^H)Fe(NCCH$_3$)$_2$] (4). Addition of 5 mL of acetonitrile to 50 mg of **2** led to an immediate color change from purple to red. Removal of the solvent in a vacuum led to the recovery of the starting material, **2**. In situ characterization clearly indicated the coordination of two acetonitrile molecules in solution. ^{1}H NMR (MeCN-d_3, 499.74 MHz): δ 7.29 (s, 4H), 7.23 (s, 4H), 6.05 (s, 4H), 0.05 (s, 12H). ^{13}C NMR (MeCN-d_3, 125.66 MHz): δ 193.4, 122.4, 119.4, 61.0, 13.4. DART HR MS (m/z): $[M-NCCH_3]^+$ 471.1918 (found), 471.1925 (calcd).

Synthesis of [(^{BMe_2,Me}TC^H)Fe(PPh$_3$)] (5). Complex **2** (100 mg, 0.23 mmol) was dissolved in 5 mL of acetonitrile in a 20 mL vial. To this purple solution, triphenyl phosphine (60. mg, 0.23 mmol) was added, which resulted in an immediate color change to yellowish brown. The solution was stirred for 15 min and was extracted three times with 5 mL of pentane to remove excess triphenylphosphine. The resulting solution was evaporated under a vacuum, and the brown solid was extracted with benzene (3 × 3 mL). The resulting solution was evaporated, yielding 90 mg of beige solid (0.13 mmol, 65% yield). ^{1}H NMR (MeCN-d_3, 499.74 MHz): δ 7.19 (s, 4H), 7.06 (t, J = 7.2 Hz, 3H), 7.00 (s, 4H), 6.92 (t, J = 7.2 Hz, 6H), 6.72 (t, J = 7.2 Hz, 6H), 5.58 (d, J = 12.3 Hz, 2H), 4.50 (d, J = 12.3 Hz, 2H), 0.20 (s, 6H), −0.14 (s, 6H). ^{13}C NMR (MeCN-d_3, 125.66 MHz): δ 196.0 (d, J = 22.5 Hz), 133.5 (d, J = 21.0 Hz), 131.5 (d, J = 8.5 Hz), 127.5, 127.3(d, J = 7.6 Hz), 123.5, 119.6, 60.5, 25.3. ^{31}P NMR (MeCN-d_3, 202.40 MHz): δ 78.7. IR: 3130, 3054, 2926, 1585, 1463, 1433, 1415, 1339, 1279, 1267, 1168, 1137, 1108, 1059, 1028, 950, 815, 800, 740, 692 cm^{-1}. DART HR MS (m/z): $[M-PPh_3]^+$ 430.1649 (found), 430.1659 (calcd) $[PPh_3+H]^+$ 260.0993 (found), 263.0990 (calcd).

Synthesis of [(^{BMe_2,Me}TC^H)Fe(CN^{t}Bu)$_2$] (6). Complex **2** (200 mg, 0.47 mmol) was dissolved in 10 mL of acetonitrile in a 20 mL vial. To the clear purple solution, *tert*-butyl isocyanide (80 mg, 0.96 mmol) was added, which resulted in an immediate color change to dark green. The solution was stirred for 15 min and extracted three times with 5 mL of pentane each to remove excess isocyanide. The resulting solution was evaporated under a vacuum, and the dark solid was extracted with benzene (3 × 5 mL). The resulting solution was evaporated, yielding 210 mg of a dark green solid (0.35 mmol, 88% yield). ^{1}H NMR (MeCN-d_3, 499.74 MHz): δ 7.16 (d, J = 1.8 Hz, 4H), 7.11 (d, J = 1.8 Hz, 4H), 5.80 (s, 4H), 0.87 (s, 18H), 0.09 (s, 12H). ^{13}C NMR (MeCN-d_3, 125.66 MHz): δ 191.9, 180.2, 123.6, 120.3, 61.4, 30.9, 14.1. IR: 3130, 2975, 2925, 2017, 1631, 1466, 1416, 1367, 1350, 1324, 1268, 1230, 1203, 1166, 1136, 1100, 1057, 1032, 953, 816, 798, 728, 692 cm^{-1}. DART HR MS (m/z): $[M]^+$ 596.3132 (found), 596.3129 (calcd).

Synthesis of [(^{BMe_2,Me}TC^H)Fe)$_2$O] (7). Complex **2** (100 mg, 0.23 mmol) was dissolved in 10 mL of benzene in a 20 mL vial. To the clear purple solution, trimethyl *N*-oxide (8.70 mg, 0.12 mmol) was added at −30 °C, which resulted in a slow color change to brown. The solution was stirred for 24 h at rt, evaporated, and extracted with THF until the residue was colorless. The resulting solution was concentrated and layered with pentane to yield brown crystals over the course of 2 weeks. The crystalline solid was washed with pentane and dried under a vacuum, yielding 65 mg (0.074 mmol, 74% yield). ^{1}H NMR (MeCN-d_3, 499.74 MHz): δ 7.13 (d, J = 1.4 Hz, 4H), 7.11 (d, J = 1.4 Hz, 4H), 5.58 (d, J = 12.0 Hz, 2H), 5.36 (d, J = 12.0 Hz, 2H), 0.41 (s, 6H), −0.67 (s, 6H). ^{13}C NMR (MeCN-d_3, 125.66 MHz): δ 179.6, 122.1, 119.5, 61.43, 15.3, 10.7. IR: 3129, 2927, 1542, 1462, 1414, 1355, 1278, 1229, 1107, 1061, 1037, 958, 816, 799, 722, 691, 659 cm^{-1}. DART HR MS (m/z): $[M]^+$ 876.3269 (found), 876.3268 (calcd).

■ ASSOCIATED CONTENT

Supporting Information

The Supporting Information is available free of charge on the ACS Publications website at DOI: 10.1021/acs.organomet.8b00923.

Additional experimental details and selected NMRs and HR MSs (PDF)

Accession Codes

CCDC 1885234−1885237 contain the supplementary crystallographic data for this paper. These data can be obtained free of charge via www.ccdc.cam.ac.uk/data_request/cif, or by emailing data_request@ccdc.cam.ac.uk, or by contacting The Cambridge Crystallographic Data Centre, 12 Union Road, Cambridge CB2 1EZ, UK; fax: +44 1223 336033.

■ AUTHOR INFORMATION

Corresponding Author

*E-mail: jenkins@ion.chem.utk.edu.

ORCID

David M. Jenkins: 0000-0003-2683-9157

Notes

The authors declare no competing financial interest.

■ ACKNOWLEDGMENTS

The authors gratefully acknowledge the National Science Foundation (NSF-CAREER/CHE-1254536) for financial support of this work. The University of Tennessee also provided additional financial support for this work via the X-ray facility.

■ REFERENCES

(1) Bass, H. M.; Cramer, S. A.; Price, J. L.; Jenkins, D. M. 18-Atom-Ringed Macrocyclic Tetra-imidazoliums for Preparation of Monomeric Tetra-carbene Complexes. *Organometallics* **2010**, *29* (15), 3235−3238.

(2) Altmann, P. J.; Weiss, D. T.; Jandl, C.; Kuehn, F. E. Exploring Coordination Modes: Late Transition Metal Complexes with a Methylene-bridged Macrocyclic Tetra-NHC Ligand. *Chem. - Asian J.* **2016**, *11* (10), 1597−1605.

(3) Fei, F.; Lu, T.; Yang, C.-F.; Chen, X.-T.; Xue, Z.-L. Synthesis, Structures, and Catalytic Properties of Dinuclear Iridium(I) Complexes with a Hexadentate Macrocyclic Diamine-Tetracarbene Ligand. *Eur. J. Inorg. Chem.* **2018**, *2018* (14), 1595−1602.

(4) Anneser, M. R.; Haslinger, S.; Poethig, A.; Cokoja, M.; Basset, J.-M.; Kühn, F. E. Synthesis and Characterization of an Iron Complex Bearing a Cyclic Tetra-N-heterocyclic Carbene Ligand: An Artificial Heme Analogue? *Inorg. Chem.* **2015**, *54* (8), 3797−3804.

(5) Altmann, P. J.; Ehrenreich, M.; Poethig, A. A hybrid imidazolylidene/imidazolium nickel NHC complex: an isolated intermediate. *Acta Crystallogr., Sect. C: Struct. Chem.* **2017**, *73* (11), 880−884.

(6) McKie, R.; Murphy, J. A.; Park, S. R.; Spicer, M. D.; Zhou, S.-z. Homoleptic crown N-heterocyclic carbene complexes. *Angew. Chem., Int. Ed.* **2007**, *46* (34), 6525−6528.

(7) Cheng, J.; Wang, L.; Wang, P.; Deng, L. High-Oxidation-State 3d Metal (Ti-Cu) Complexes with N-Heterocyclic Carbene Ligation. *Chem. Rev.* **2018**, *118* (19), 9930−9987.

(8) Jain, K. R.; Herrmann, W. A.; Kuehn, F. E. High oxidation state transition metal complexes ligated with N-heterocyclic carbenes. *Curr. Org. Chem.* **2008**, *12* (17), 1468−1478.

(9) Jahnke, M. C.; Ekkehardt Hahn, F. Chapter 1 Introduction to N-Heterocyclic Carbenes: Synthesis and Stereoelectronic Parameters. *N-Heterocyclic Carbenes: From Laboratory Curiosities to Efficient Synthetic Tools*; The Royal Society of Chemistry: 2011; pp 1−41.

DOI: 10.1021/acs.organomet.8b00923
Organometallics XXXX, XXX, XXX−XXX

(10) Riener, K.; Haslinger, S.; Raba, A.; Hoegerl, M. P.; Cokoja, M.; Herrmann, W. A.; Kuehn, F. E. Chemistry of Iron N-Heterocyclic Carbene Complexes: Syntheses, Structures, Reactivities, and Catalytic Applications. *Chem. Rev.* **2014**, *114* (10), 5215−5272.
(11) Hahn, F. E.; Langenhahn, V.; Luegger, T.; Pape, T.; Le Van, D. Template synthesis of a coordinated tetracarbene ligand with crown ether topology. *Angew. Chem., Int. Ed.* **2005**, *44* (24), 3759−3763.
(12) Radloff, C.; Gong, H.-Y.; Schulte to Brinke, C.; Pape, T.; Lynch, V. M.; Sessler, J. L.; Hahn, F. E. Metal-Dependent Coordination Modes Displayed by Macrocyclic Polycarbene Ligands. *Chem. - Eur. J.* **2010**, *16* (44), 13077−13081.
(13) Kupper, C.; Rees, J. A.; Dechert, S.; DeBeer, S.; Meyer, F. Complete Series of $\{FeNO\}^8$, $\{FeNO\}^7$, and $\{FeNO\}^6$ Complexes Stabilized by a Tetracarbene Macrocycle. *J. Am. Chem. Soc.* **2016**, *138* (25), 7888−7898.
(14) Meyer, S.; Klawitter, I.; Demeshko, S.; Bill, E.; Meyer, F. A Tetracarbene-Oxoiron(IV) Complex. *Angew. Chem., Int. Ed.* **2013**, *52* (3), 901−905.
(15) Cramer, S. A.; Jenkins, D. M. Synthesis of Aziridines from Alkenes and Aryl Azides with a Reusable Macrocyclic Tetracarbene Iron Catalyst. *J. Am. Chem. Soc.* **2011**, *133* (48), 19342−19345.
(16) Chandrachud, P. P.; Bass, H. M.; Jenkins, D. M. Synthesis of Fully Aliphatic Aziridines with a Macrocyclic Tetracarbene Iron Catalyst. *Organometallics* **2016**, *35* (11), 1652−1657.
(17) Kueck, J. W.; Anneser, M. R.; Hofmann, B.; Poethig, A.; Cokoja, M.; Kuehn, F. E. Fighting Fenton Chemistry: A Highly Active Iron(III) Tetracarbene Complex in Epoxidation Catalysis. *ChemSusChem* **2015**, *8* (23), 4056−4063.
(18) Bass, H. M.; Cramer, S. A.; McCullough, A. S.; Bernstein, K. J.; Murdock, C. R.; Jenkins, D. M. Employing Dianionic Macrocyclic Tetracarbenes To Synthesize Neutral Divalent Metal Complexes. *Organometallics* **2013**, *32* (7), 2160−2167.
(19) Do-Thanh, C.-L.; Khanal, N.; Lu, Z.; Cramer, S. A.; Jenkins, D. M.; Best, M. D. Chloride binding by a polyimidazolium macrocycle detected via fluorescence, NMR, and X-ray crystallography. *Tetrahedron* **2012**, *68* (6), 1669−1673.
(20) Cramer, S. A.; Sturgill, F. L.; Chandrachud, P. P.; Jenkins, D. M. Overcoming NHCs neutrality: installing tetracarbenes on group 13 and 14 metals. *Dalton Trans.* **2014**, *43* (21), 7687−7690.
(21) Kupper, C.; Schober, A.; Demeshko, S.; Bergner, M.; Meyer, F. An Exclusively Organometallic $\{FeNO\}^7$ Complex with Tetracarbene Ligation and a Linear FeNO Unit. *Inorg. Chem.* **2015**, *54* (7), 3096−3098.
(22) Montagne, C.; Shipman, M. Modified Bucherer-Bergs reaction for the one-pot synthesis of 5,5′-disubstituted hydantoins from nitriles and organometallic reagents. *Synlett* **2006**, *2006*, 2203−2206.
(23) Pascualini, M. E.; Di Russo, N. V.; Thuijs, A. E.; Ozarowski, A.; Stoian, S. A.; Abboud, K. A.; Christou, G.; Veige, A. S. A high-spin square-planar Fe(II) complex stabilized by a trianionic pincer-type ligand and conclusive evidence for retention of geometry and spin state in solution. *Chem. Sci.* **2015**, *6* (1), 608−612.
(24) Scheidt, W. R.; Reed, C. A. Spin-state/stereochemical relationships in iron porphyrins: implications for the hemoproteins. *Chem. Rev.* **1981**, *81* (6), 543−55.
(25) Yang, L.; Powell, D. R.; Houser, R. P. Structural variation in copper(I) complexes with pyridylmethylamide ligands: structural analysis with a new four-coordinate geometry index, τ_4. *Dalton Trans.* **2007**, *9*, 955−964.
(26) Haslinger, S.; Lindhorst, A. C.; Kueck, J. W.; Cokoja, M.; Poethig, A.; Kuehn, F. E. Isocyanide substitution reactions at the trans labile sites of an iron(II) N-heterocyclic carbene complex. *RSC Adv.* **2015**, *5* (104), 85486−85493.
(27) Wang, L.; Cheng, J.; Deng, L. A square planar iron(II) biphenyl-2,2′-diyl complex with NHC ligation: Synthesis, characterization, and its reactivity toward unsaturated organic substrates. *Inorg. Chim. Acta* **2017**, *460*, 49−54.
(28) Cronin, D. L.; Wilkinson, J. R.; Todd, L. J. Carbon-13 NMR study of isonitrile transition metal complexes. *J. Magn. Reson.* **1975**, *17* (3), 353−61.
(29) Liang, Q.; Salmon, A.; Kim, P. J.; Yan, L.; Song, D. Unusual Rearrangement of an N-Donor-Functionalized N-Heterocyclic Carbene Ligand on Group 8 Metals. *J. Am. Chem. Soc.* **2018**, *140* (4), 1263−1266.
(30) Anneser, M. R.; Haslinger, S.; Poethig, A.; Cokoja, M.; D'Elia, V.; Hoegerl, M. P.; Basset, J.-M.; Kuehn, F. E. Binding of molecular oxygen by an artificial heme analogue: investigation on the formation of an Fe-tetracarbene superoxo complex. *Dalton Trans.* **2016**, *45* (15), 6449−6455.
(31) Doyle, M. P. Catalytic methods for metal carbene transformations. *Chem. Rev.* **1986**, *86* (5), 919−40.
(32) Gopalaiah, K. Chiral Iron Catalysts for Asymmetric Synthesis. *Chem. Rev.* **2013**, *113* (5), 3248−3296.
(33) Courtemanche, M.-A.; Transue, W. J.; Cummins, C. C. Phosphinidene Reactivity of a Transient Vanadium P≡N Complex. *J. Am. Chem. Soc.* **2016**, *138* (50), 16220−16223.
(34) Rankin, M. A.; Cummins, C. C. Terminal phosphinidene formation via tantalaziridine complexes. *Dalton Trans.* **2012**, *41* (32), 9615−9618.
(35) Transue, W. J.; Velian, A.; Nava, M.; Garcia-Iriepa, C.; Temprado, M.; Cummins, C. C. Mechanism and Scope of Phosphinidene Transfer from Dibenzo-7-phosphanorbornadiene Compounds. *J. Am. Chem. Soc.* **2017**, *139* (31), 10822−10831.
(36) Marinetti, A.; Mathey, F. The carbene-like behavior of terminal phosphinidene complexes toward olefins. A new access to the phosphirane ring. *Organometallics* **1984**, *3* (3), 456−61.
(37) Mathey, F. Phospha-organic chemistry: Panorama and perspectives. *Angew. Chem., Int. Ed.* **2003**, *42* (14), 1578−1604.
(38) Jikyo, T.; Maas, G. Different thermal reactivity of a 1,2-thiaphospholo[a]phosphirane in free and metal carbonyl complexed form. *Chem. Commun.* **2003**, *22*, 2794−2795.
(39) Shimizu, T.; Miyasaka, D.; Kamigata, N. Reaction of 1,3-Bis(alkylseleno)allenes with Diphenyl Diazomethane. *J. Org. Chem.* **2001**, *66* (21), 7202−7204.
(40) Velian, A.; Cummins, C. C. Facile Synthesis of Dibenzo-7λ3-phosphanorbornadiene Derivatives Using Magnesium Anthracene. *J. Am. Chem. Soc.* **2012**, *134* (34), 13978−13981.
(41) Schisler, A.; Loennecke, P.; Gelbrich, T.; Hey-Hawkins, E. The reactivity of *cyclo*-$(P_5{}^tBu_4)$- towards group 13, 14 and 15 metal chlorides: complexation and formation of cyclooligophosphanes, $\{cyclo\text{-}(P_5{}^tBu_4)\}_2$ and $\{cyclo\text{-}(P_4{}^tBu_3)P^tBu\}_2$, by reductive elimination. *Dalton Trans.* **2004**, *18*, 2895−2898.

DOI: 10.1021/acs.organomet.8b00923
Organometallics XXXX, XXX, XXX−XXX